

# Statistical Description in the Turbulent Near Wake of a Rotating Circular Cylinder

Sharul S. Dol, U. Azimov, Robert J. Martinuzzi

**Abstract**—Turbulence studies were made in the wake of a rotating circular cylinder in a uniform free stream. The interest was to examine the turbulence properties at the suppression of periodicity in vortex formation process. An experimental study of the turbulent near wake of a rotating circular cylinder was made at a Reynolds number of 9000 for velocity ratios,  $\lambda$  between 0 and 2.7. Hot-wire anemometry and particle image velocimetry results indicate that the rotation of the cylinder causes significant changes in the vortical activities. The turbulence quantities are getting smaller as  $\lambda$  increases due to suppression of coherent vortex structures.

**Keywords**—rotating circular cylinder, Reynolds stress, vortex

## I. INTRODUCTION

The study of vortices (i.e. vortex dynamics) leads to an understanding of turbulent flow. Turbulence is rotational and characterized by high levels of fluctuating vorticity. For this reason, vortex dynamics plays an essential role in the description of turbulent flows. For example, the existence of energy transfer (i.e. energy cascade) from large eddies to small eddies is driven by vortex-stretching mechanism [1]. This is an important concept to explain why turbulent flows are dissipative.

There has been interest in the vortical instabilities in wakes since the early experiments of Strouhal in 1878. However, it was not until [2] produced his first paper on the theory of vortex streets that the research exploded because of the practical importance to engineers (e.g. the jumbo jet wake hazard phenomenon, the wakes of submarines), as well as to scientists (e.g. the wake of the earth in the solar wind, cumulus clouds are in turbulent motion).

The formation of vortices in the wake is generally considered to be the result of Kelvin-Helmholtz instabilities (i.e. shear flow instability), causing the equally intense, but oppositely signed, shear layers to roll up. Kelvin-Helmholtz instability is the instability at the interface between two horizontal parallel streams of different velocities and densities that a steady, disturbed state is not possible and pressure gradients are in directions which amplify the disturbance. The source of energy for generating the instability is derived from the kinetic energy of the shear flow. Some descriptive information of near wake vortex formation comes from the instantaneous-streamline patterns described by [3].

S. S. Dol is with the Curtin University, Miri, Sarawak, MALAYSIA (phone: 085-443830; fax: 085-443837; e-mail: sharulsham@curtin.edu.my).

U. Azimov is with the Curtin University, Miri, Sarawak, MALAYSIA (e-mail: u.azimov@curtin.edu.my).

R. J. Martinuzzi is with the University of Calgary, Calgary, Alberta, CANADA (e-mail: rmartinu@ucalgary.ca).

Rotation of the cylinder can substantially alter the behaviour of the wake with respect to the stationary case, due to the modification in the upper and lower boundary layers and separated shear layers.

The flow field depends primarily on two parameters. The first is the velocity ratio,

$$\lambda = \frac{U_P}{U_\infty} \quad (1)$$

where

$$U_P = \frac{\Omega D}{2} \quad (2)$$

is the surface speed of the cylinder,  $U_\infty$  is the freestream velocity,  $\Omega$  is the angular speed of the rotation and  $D$  is the cylinder diameter. The second is the Reynolds number,

$$Re = \frac{U_\infty D}{\nu} \quad (3)$$

where  $\nu$  is the kinematic viscosity of the fluid.

The main objectives of the present work were first; to quantify statistically the turbulence quantities in the near wake region of a rotating cylinder flow and second; to study the rotational effects to the generation of turbulence stresses. The analysis was used to investigate vortex formation and interaction in the near wake region that could provide answers to weaker vortices for the rotating case.

## I. EXPERIMENTAL DETAILS

The experiments were performed at the Boundary Layer Wind Tunnel Laboratory (BLWTL) of the University of Western Ontario (UWO) in a suction-type wind tunnel with a 1500 mm long working section and a 450 x 450 mm<sup>2</sup> cross section. Hot-wire anemometry (HWA) measurements across the test section showed a uniform free-stream and a turbulence intensity of less than 1%. A smooth steel circular cylinder of nominal diameter  $D = 24$  mm was mounted horizontally in the midplane spanning the full width of the working section. A photograph of the set-up is shown in Fig. 1. The cylinder aspect ratio was about 18.8 so that the statistical properties of the flow were effectively two-dimensional [4]. The blockage ratio was 5.3%, which is at the upper bound of the region of negligible blockage effects [5 and 6]; no correction was made for blockage effects. A definition sketch of the flow is given in [7]. HWA and particle image velocimetry (PIV) experiments were performed at Reynolds number of 9000 and for speed ratios,  $\lambda$ , between 0 and 2.7. Operating parameters for the HWA and PIV set-up and measurements can be found in [7].

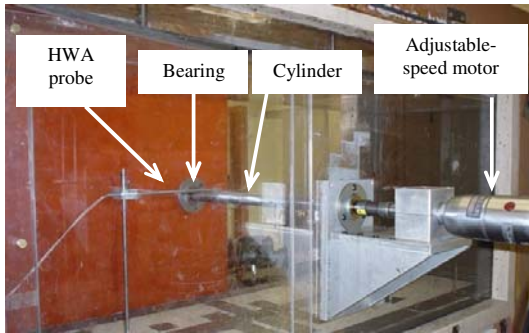


Figure 1. A photograph showing the mechanical set-up.

## II. THE STATISTICAL DESCRIPTION OF TURBULENT WAKES

The variables in a turbulent flow are not deterministic in details and have to be treated as stochastic or random variables. It is important to examine how fluctuations are distributed around an average value and how adjacent fluctuations are related. Turbulence contains a wide range of different scales or sizes of eddies, which co-exists giving a continuum of scales that may be treated statistically. Statistical properties of an ensemble of realizations were used to obtain useful quantities (i.e. averages, probability density functions). To do this, the flow was split into a mean part and a fluctuating component. The latter may be taken to represent the turbulence.

The statistical description of turbulence (Table 1) was determined from the streamwise velocity time series in the near wake, using a single normal hot-wire connected to a DANTEC constant-temperature anemometry (CTA) system. Signals from the circuits were offset, amplified and low-pass filtered at half of the sampling rate. The sampling rate was 5000 Hz. The duration of each record was 60 seconds. Experiments were performed at Reynolds number of 9000 and for speed ratios,  $\lambda$ , between 0 and 2.7.

The average centerline velocities represent the maximum velocity deficit of the wake,  $U_c$ . The non-dimensionalized centerline velocity,  $U_c/U_\infty$ , for the stationary cylinder is 0.67. This velocity defect is due to the vortex interaction in the wake (i.e. rapid diffusion of the mean flow) and these rotational activities slow down the fluid particles, causing drag. The velocity defect profile is self-preserving [8]. The centerline velocity defect decays inversely with the square root of the streamwise distance [1]. The entrainment of the surrounding fluid increases the mass flux across the wake resulting in reduction of turbulent fluctuation behind the cylinder in the far wake region. The velocity defect is smaller as  $\lambda$  increases.  $U_c/U_\infty$  is about unity when  $\lambda \geq 2.0$ . This is due to the reduced vortex activity in the formation region [7]. This also implies that the location at which the maximum velocity defects is shifted.

The mean square value, the variance (or the rms value of the fluctuation, the standard deviation) becomes smaller at higher rotational rates (especially when  $\lambda \geq 2.0$ ). This also

means that the width of the probability density function becomes smaller (i.e. turbulent fluctuations are reduced into the vicinity of the mean value). Consequently, the turbulent intensities,  $Ti$  are also getting smaller as  $\lambda$  increases due to suppression of coherent vortex structures.

Skewness, which is a non-dimensionalized third moment, is a measure of the asymmetry of the distribution around the sample mean. Many classical turbulent statistical tests depend on normality assumptions. Significant skewness indicates that data are not normal. Skewness also implies growth in the surface area of a sheet at which vorticity differs than zero. The distribution is said to be right-skewed (left-skewed) if the mass of the distribution is concentrated to the left (right). The measure of skewness results in negative values for all velocity ratios so that the data are spread out more to the right side of the mean. This negative skewness is believed to be related to the vortex folding and stretching process. The skewness for  $\lambda = 2.7$  indicates the highest deviation.

Kurtosis, which is a non-dimensionalized fourth moment, is a measure of how outlier-prone a distribution is. The kurtosis of the normal distribution is 3. Higher kurtosis means more of the variance is due to infrequent extreme deviations. The kurtosis for  $\lambda = 2.7$  shows large value. This is probably due to the intermittency of vortex shedding process as described by [7].

TABLE I STATISTICAL RESULT

$\lambda$	$U_{\text{mean}}$ (m/s)	rms	Variance	$Ti$ (%)	Skewness	Kurtosis
0	3.81	1.71	2.93	30.02	-0.20	-0.63
0.5	4.72	1.49	2.21	26.06	-0.44	-0.02
1.0	4.87	1.23	1.51	21.58	-0.68	0.39
1.5	4.96	0.95	0.89	16.58	-0.45	0.04
2.0	5.12	0.80	0.64	14.05	-0.83	1.22
2.7	5.27	0.40	0.16	6.99	-1.44	9.55

## III. THE REYNOLDS STRESS

The flow past a rotating cylinder has been studied extensively [4, 9, 10, 11, 12 and 13], yet much continues to be unknown about the flow structure and dynamics of this geometrically simple, turbulent flow. Vortical structures in the flow and their interactions are believed to play an important role in the generation of turbulent stresses, turbulent kinetic energy, wake entrainment and growth and mean flow development. However, the direct and correct identification and observation of vortical structures and their interactions when the cylinder rotates has received little attention to date. The in-plane Reynolds stress distributions were obtained to study the flow physics and structure of vortices.

The  $x$ - $y$  plane Reynolds stress components  $\overline{u^2}$ ,  $\overline{v^2}$  and  $-\overline{uv}$  for a stationary cylinder case are shown in Fig. 2. In the region where the vortices begin to be convected, the highest values of the normal stresses are located near the center of the vortices while the highest values of the shear stress are located between the vortices in the saddle regions. In the very near region characterized by the formation of the vortices, high values of  $\langle u^2 \rangle$  and  $\langle uv \rangle$  are located in the separated shear layer, as expected. These high values then follow the motion of the vortices and are transported towards the center of the wake. It is also noticeable that significant values of  $\langle v^2 \rangle$  are found in the regions connecting the vortices. This is presumably due to the presence of longitudinal vortices, connecting the primary ones. It shows that vortex pairing events are undoubtedly associated with Reynolds stresses in the flow.

Cantwell and Coles [14] measured various quantities relevant to the Reynolds stresses for the  $Re = 1.4 \times 10^5$  flow. Reynolds stress receives contribution from both the random and periodic motion of the flow. They observed that the contribution of the random turbulent fluctuations, to the Reynolds stress is much larger than that from the organized large eddies. The results indicate that the Reynolds stresses are symmetric about the center axis and the normal components are in general, larger than the shear components. Similar to the observations of [14], it is seen that  $\langle v^2 \rangle$  field achieves a peak along the center axis while the peaks in  $\langle u^2 \rangle$  and  $\langle uv \rangle$  are achieved off the flow axis, within the wake bubble.

Reynolds stresses are found to remain at significant levels after the formation region. This suggests continuing vortex activity in the vortex street and this can be seen in the instantaneous vorticity fields in Fig 2d. The relatively large scales of these vortex packets in the wake lead to the suggestion that large-scale structures are responsible for the production of turbulent stresses. Peak values of the Reynolds stresses are listed in Table 2. The symmetry of the peak values implies a typical Kármán vortex shedding pattern of alternating vortices with the same strength advancing downstream. The general topology of these stresses is found in good agreement with the vorticity contour plot and vortex core identification of [7].

TABLE 2 PEAK VALUES OF THE REYNOLDS STRESSES

$\lambda$	$-\overline{uv}/U_\infty^2 \times 100$	$\overline{u^2}/U_\infty^2 \times 100$	$\overline{v^2}/U_\infty^2 \times 100$
0	$\pm 11.0$	27.7	32.9
2.0	5.6 (upper) -8.1 (lower)	11.0	15.1

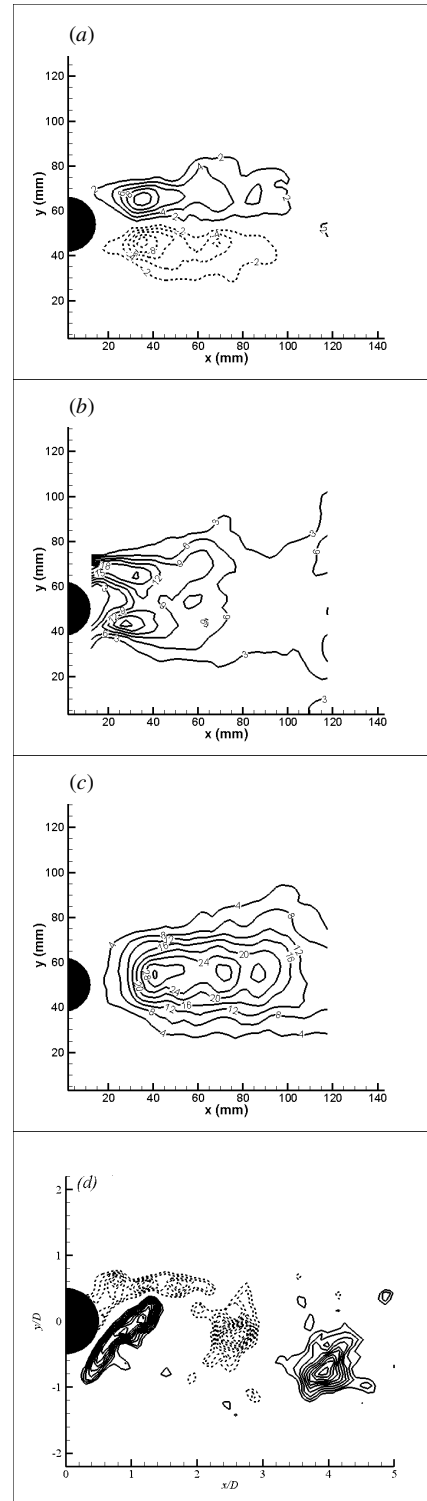


Figure 2. Reynolds stress distributions in the  $x$ - $y$  plane for  $\lambda = 0$   
 (a)  $-\overline{uv}/U_\infty^2 \times 100$  (b)  $\overline{u^2}/U_\infty^2 \times 100$  (c)  $\overline{v^2}/U_\infty^2 \times 100$   
 (d) instantaneous vorticity contours.

The  $x$ - $y$  plane Reynolds stress components  $\overline{u^2}$ ,  $\overline{v^2}$  and  $-\overline{uv}$  for  $\lambda = 2.0$  are shown in Fig. 3. The location for the peak turbulent stresses follow similar pattern as the non-rotating case. However, the peak values of the Reynolds stresses are much smaller (about 60% less), as shown in Table 2. The normal components are still larger than shear component. Rotation of the cylinder induces asymmetry to the flow field. The  $\langle uv \rangle$  value for the lower vortex is larger than the one in the upper vortex. This is probably because the vertical component velocity within the formation region below the centerline is more affected by the rotation [7]. The effect of rotation causes the upward wake deflection. The peak value of  $\langle u^2 \rangle$  is formed at the upper shear layer. This is probably because the rotation of the cylinder has the opposite sense to the free stream at that region. When the surface is traveling with the free-stream velocity, the transition can be expected to be delayed, and conversely. The boundary layer behavior can then be correlated with a relative Reynolds number and a qualitative estimation of the relative portions of laminar and turbulent boundary layer and total length of boundary layer can be obtained. Due to the opposing motion between the wall and the free-stream, the upper relative Reynolds number increases, and conversely [15]. This signifies a longer attached boundary layer on the top than on the bottom. At higher rotational speeds, a greater portion of the upper boundary layer becomes turbulent and therefore more re-attached. It is also seen that  $\langle v^2 \rangle$  field achieves a peak along the center axis. Generally, as  $\lambda$  increases the vortex cores are increasingly deflected in positive lateral direction and the separation between upper and lower vortices becomes smaller. The present observations are consistent with the plot of vorticity contours.

There is a difference in vorticity strength between the vortices shed from the upper and lower sides of the cylinder. Unlike the classical shedding process, the vortices are not completely shed from the base of the cylinder. There are bound vortices at the base on the upper and lower sides of the cylinder and only part of the circulation (i.e. part of the vortex) is shed during each cycle. The bound vortex would thus interfere with the separation streamline at the surface of the cylinder and reduce the net rate of circulation flux, resulting in weaker vortices [7 and 16]. Although alternate vortex shedding appears, it is difficult to observe Kármán vortex street in the wake. Fig. 3d shows the distorted street, which at certain points, the positions of clockwise and counter-clockwise vortices are interchanged with the former one appears at the lower layer and vice versa as they are convected downstream.

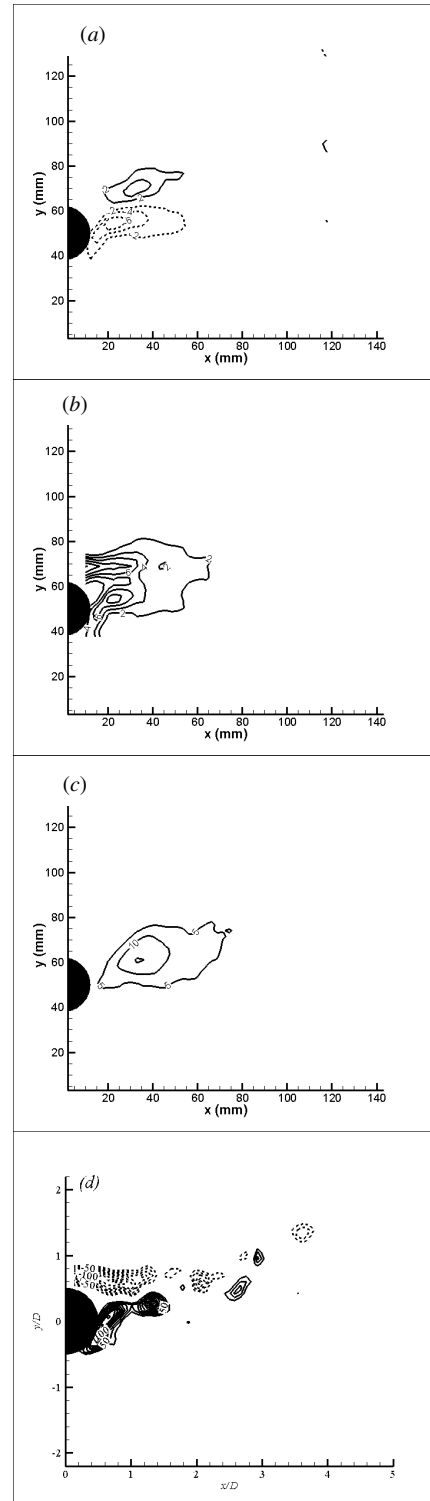


Figure 3. Reynolds stress distributions in the  $x$ - $y$  plane for  $\lambda = 2.0$   
 (a)  $-\overline{uv} / U_\infty^2 \times 100$  (b)  $\overline{u^2} / U_\infty^2 \times 100$  (c)  $\overline{v^2} / U_\infty^2 \times 100$   
 (d) instantaneous vorticity contours.

## IV. CONCLUSION

The results obtained in the present study establish that shedding of Kármán vortices in a rotating circular cylinder-generated wake is modified by rotation of the cylinder. Alternate vortex shedding is highly visible when  $\lambda < 2.0$  although the strength of the separated shear layers differ due to the rotation of the cylinder. The statistics and turbulence quantities in the wakes show significant changes at  $\lambda = 2.0$ . The results indicate that the rotation of the cylinder causes significant disruption in the structure of the flow. It is clear that flow asymmetries will weaken vortex shedding, and when the asymmetries are significant enough, total suppression of a periodic street occurs.

## ACKNOWLEDGMENT

This research was partially funded by the Natural Science and Engineering Research Council of Canada. Equipment was obtained through grants from the Canada Foundation for Innovation, the Ontario Innovation Trust, and the UWO Academic Development Fund.

## REFERENCES

- [1] Tennekes, H. and Lumley, J.L. (1972). *A First Course in Turbulence*. MIT Press, Massachusetts.
- [2] Kármán, Th von. (1912). Über den mechanismus den widerstands, den ein bewegter körper in einer flüssigkeit erfährt. *Göttingen Nachr. Math. Phys. Kl.* Vol. 12, pp. 509.
- [3] Perry, A.E., Chong, M.S. and Lim, T.T. (1982). The vortex-shedding process behind two-dimensional bluff bodies, *Journal of Fluid Mechanics*, Vol. 116, pp. 77.
- [4] Massons, J., Ruiz, X. and Diaz, F. (1989). Image processing of the near wakes of stationary and rotating cylinders, *Journal of Fluid Mechanics*, Vol. 204, pp. 167.
- [5] West, G.S. and Apelt, C.J. (1982). The effects of tunnel blockage and aspect ratio on the mean flow past a circular cylinder with Reynolds number between  $10^4$  and  $10^5$ , *Journal of Fluid Mechanics*, Vol. 114, pp. 361.
- [6] Laneville, A. (1990). Turbulence and blockage effects on two dimensional rectangular cylinders, *Journal of Wind Engineering and Industrial Aerodynamics*, Vol. 33, pp. 11.
- [7] Dol, S.S., Kopp, G.A. and Martinuzzi, R.J. (2008). The suppression of periodic vortex shedding from a rotating circular cylinder, *Journal of Wind Engineering and Industrial Aerodynamics*, 96, pp.1164–1184.
- [8] Kundu P.K. and Cohen I.M. (2004). *Fluid Mechanics*. Elsevier Academic Press, San Diego.
- [9] Diaz, F., Gavalda, J., Kawall, J.G., Keffer, J.F. and Giralt, F. (1983). Vortex shedding from a spinning cylinder, *Physics of Fluids*, Vol. 26, pp. 3454.
- [10] Badr, H.M., Coutanceau, M., Dennis, S.C.R. and Menard, C. (1990). Unsteady flow past a rotating circular cylinder at Reynolds number  $10^3$  and  $10^4$ , *Journal of Fluid Mechanics*, Vol. 220, pp. 459.
- [11] Chang, C.C. and Chern, R.L. (1991). Vortex shedding from an impulsively started rotating and translating circular cylinder, *Journal of Fluid Mechanics*, Vol. 233, pp. 265.
- [12] Tokumaru, P.T. and Dimotakis, P.E. (1991). Rotary oscillatory control of a cylinder wake, *Journal of Fluid Mechanics*, Vol. 224, pp. 77.
- [13] Chew, Y.T., Cheng, M. and Luo, S.C. (1995). A numerical study of flow past a rotating circular cylinder using a hybrid vortex scheme, *Journal of Fluid Mechanics*, Vol. 299, pp. 35.
- [14] Cantwell, B. and Coles, D. (1983). An experimental study of entrainment and transport in the turbulent near wake of a circular cylinder, *Journal of Fluid Mechanics*, Vol. 136, pp. 321.
- [15] Swanson, W.M. (1961). The Magnus effect: A summary of investigations to date, *Journal of Basic Engineering*, Vol. 83, pp. 461.
- [16] Dol, S.S. and Martinuzzi, R.J. (2012). Patterns of vortex shedding from a rotating cylinder, Proceedings of 7<sup>th</sup> CUTSE Conference, Curtin University, Sarawak.